LBNL-54411

Report Title

CO_2 Capture Project - An Integrated, Collaborative Technology Development Project for Next Generation CO_2 Separation, Capture and Geologic Sequestration

HSE Risk Assessment of Deep Geological Storage Sites

Report Reference
2.1.3

Type of Report:	Final Report
Reporting Period Start Date:	April 2001
Reporting Period End Date:	November 2003
Principal Author(s):	Curtis M. Oldenburg, André A. J. Unger, Yingqi Zhang, Jennifer L. Lewicki
Date Report was issued:	December 2003
Submitting Organization:	Lawrence Berkeley National Laboratory
Address:	Earth Sciences Division 90-1116 1 Cyclotron Rd. Berkeley, CA 94720

2.1.3.1 Abstract

The injection of carbon dioxide (CO_2) into deep geologic carbon sequestration sites entails risk that CO_2 will leak away from the primary storage target formation and migrate upwards where it can seep out of the ground. We have developed and applied a coupled modeling framework called T2CA for simulating CO_2 leakage and seepage in the subsurface and in the atmospheric surface layer for risk characterization. The results of model simulations can be used to quantify the two key health, safety, and environmental (HSE) risk drivers, namely CO_2 seepage flux and near-surface CO_2 concentrations. The methodology and structure of the coupled modeling framework are based on the concepts that (1) the primary HSE risk is in the near-surface environment where humans, animals, and plants live, (2) leakage and seepage flow processes are coupled, and (3) the main risk drivers are CO_2 flux and concentration. The coupled modeling framework T2CA is built on the integral finite difference multiphase and multicomponent reservoir simulator TOUGH2 and models CO_2 and air in both subsurface and atmospheric surface-layer regions simultaneously. In the surface-layer, winds are assumed to follow a logarithmic velocity profile and the advection and dispersion are assumed to be passive, i.e., not density-dependent. We use parameterized surface-layer dispersivities calculated from the Pasquill-Gifford curves and Smagorinski Model. We have verified T2CA on the basis of gas-mixture physical property prediction, surface-layer transport and dispersion, and transition from passive to active flow. Sensitivity studies for a subsurface system with a thick unsaturated zone show limited leakage attenuation resulting in correspondingly large CO_2 concentrations in the shallow subsurface. Large CO_2 concentrations in the shallow subsurface present a risk to plants and their roots, and to humans and other animals in subsurface openings such as basements or utility vaults. We demonstrate the model for a coupled subsurface–surface-layer system and show that seeping CO_2 can reflux into the subsurface as a dissolved component in infiltrating rainwater. Whereas CO_2 concentrations in the subsurface are high, surface-layer winds reduce CO_2 concentrations to low levels for the fluxes investigated. Application of T2CA to the Rio Vista Gas Field in California shows that the windy conditions of the present climate regime at Rio Vista are capable of dispersing significant CO_2 seepage fluxes. We recommend more applications and case studies be carried out with T2CA, along with the development of extensions to handle additional scenarios such as calm conditions, topographic effects, and catastrophic surface-layer discharge events.

2.1.3.2 Table of Contents

2.1.3.3 List(s) of Graphical Materials

2.1.3.4 Introduction

The injection of carbon dioxide (CO_2) into deep geologic formations for carbon sequestration involves the risk that CO_2 will unexpectedly leak away from the target formation and migrate generally upward eventually reaching the shallow subsurface where CO_2 could seep out of the ground. In the near-surface environment, high concentrations of CO_2 can pose significant health, safety, and environmental (HSE) risks. The assessment of HSE risks is an essential part of public acceptance, planning, and permitting of geologic carbon sequestration projects. Risk assessment in general can be divided into three parts: (1) definition of scenarios of what can go wrong; (2) assessment of the likelihood of those scenarios; and (3) assignment of a measure of severity to the consequences arising from a given scenario. When applying this approach to substances that pose a hazard to human health and ecosystems, the risk assessment process includes hazard identification and risk characterization. For geologic carbon sequestration, a recognized HSE hazard is CO_2 leakage and seepage from the storage site leading potentially to exposure by humans, plants, and animals to elevated CO_2 concentrations in air and water. Risk characterization requires the estimation or calculation of elevated CO_2 concentrations to which humans, plants, and animals may be exposed in the given failure scenarios. The research described here focuses on estimating CO_2 concentrations and fluxes by using a coupled subsurface and atmospheric-surface-layer numerical simulator.

A formal and consistent terminology to describe the different modes of CO_2 migration. We define *leakage* as migration away from the primary sequestration target formation, whereas *seepage* is CO_2 migration through an interface such as the ground surface, a basement floor or wall, or the bottom of a body of surface water. In Figure 2.1.3.4(1), we present a schematic of some of the important features that may affect HSE risk characterization for CO_2 leakage and seepage in the shallow subsurface and atmospheric surface layer. These features include a house with a basement and cracked floor through which CO_2 can seep, and a water well which could produce water with high dissolved CO_2 content if CO_2 leaked up through the aquifer. Also shown are plants, a tree, and roots that may be sensitive to elevated CO_2 concentrations in the shallow subsurface. We also show animals that live in the ground and therefore may be susceptible to elevated CO_2 concentrations, along with their burrows that may provide fast-flow paths for CO_2 that enhance mixing by barometric pumping of soil gas and ambient atmosphere. In addition, we show in Figure 2.1.3.4(1) the saturated zone, unsaturated zone, surface water, and wind in the atmospheric surface layer all of which may be capable of diluting and attenuating leaking and seeping CO_2.

The objective of our research is to demonstrate a coupled modeling framework for risk characterization applicable to the leakage and seepage of CO_2 from geologic carbon sequestration sites. The purpose of the coupled model is to estimate CO_2 fluxes and concentrations in the near-surface environment where risk to humans, plants, and animals is highest. The underlying premise of our approach is that the fundamental drivers of the HSE risk are the CO_2 flux and near-surface CO_2 concentrations, and that a rigorous capability to estimate these quantities is essential for a defensible HSE risk assessment. A new coupled model is required because to our knowledge there is no existing model that handles both subsurface and atmospheric surface-layer transport and dispersion along with the coupling at the subsurface–surface-layer interface at length scales of order 10^2–10^3 m. The focus of T2CA is on diffuse and low level leakage that could occur through the natural barriers in the subsurface as opposed to catastrophic leakage such as may occur through abandoned wells or well blowouts.

The purpose of this report is to summarize our research effort into the development, testing, and application of the coupled modeling framework T2CA over the last one and one-half years. This work has been described in detail in five project deliverable reports (Oldenburg et al., 2002a; Oldenburg et al., 2002b; Oldenburg et al., 2002c; Oldenburg and Unger, 2003b, and Oldenburg et al., 2003a) and two publications (Oldenburg and Unger, 2003c; and Oldenburg and Unger, 2003d) to which readers interested in greater detail can refer.

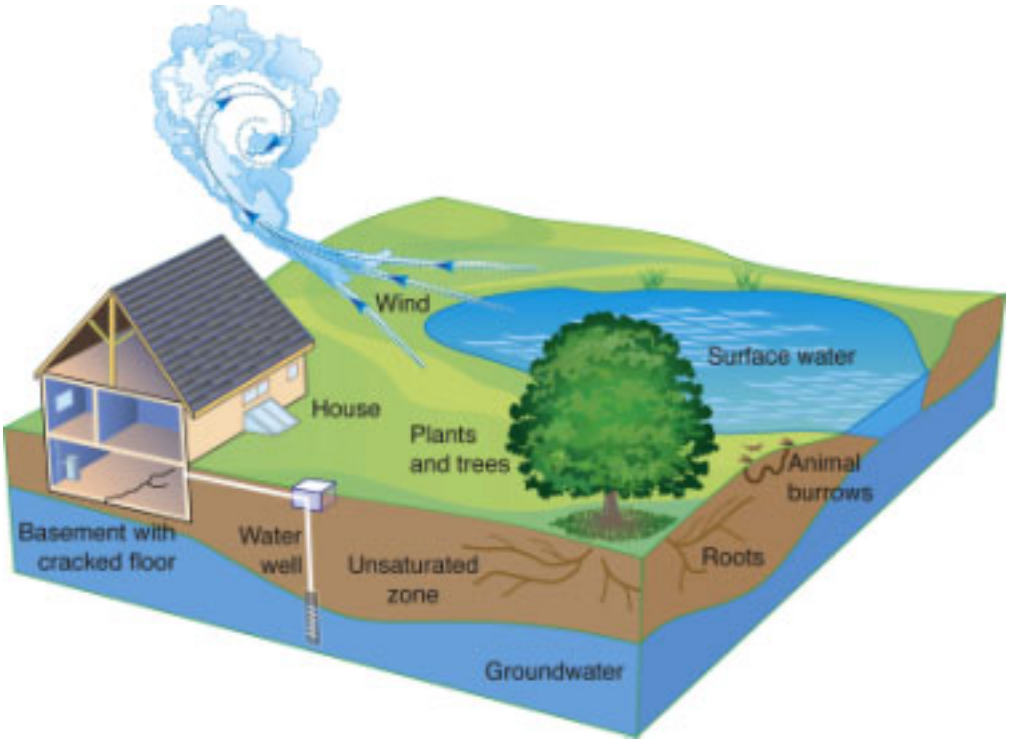

Figure 2.1.3.4(1). Sketch of near-surface environment with accompanying features relevant to HSE risk associated with CO_2 leakage and seepage

2.1.3.5 Executive Summary

The injection of carbon dioxide (CO_2) into deep geologic sequestration sites entails risk that CO_2 will leak away from the primary storage target formation and potentially migrate upwards where it can seep out of the ground. Hazard identification and risk characterization are essential components of health, safety, and environmental (HSE) risk assessment of geologic carbon sequestration. The hazard of concern is exposure to elevated CO_2 concentrations resulting from leakage and seepage of CO_2 from the geologic sequestration site. Risk characterization is the quantification of the significance of this hazard, and includes estimating source strength and environmental concentrations in media through which exposure to CO_2 by humans, plants, and animals may occur. We describe here a coupled modeling framework for simulating CO_2 leakage and seepage, including transport and dispersion in the subsurface and in the atmospheric surface layer, for risk characterization. *Leakage* is defined as migration away from the primary storage formation, while *seepage* is flow across a boundary such as the ground surface.

The methodology and structure of the coupled modeling framework are based on the key concepts that (1) the primary HSE risk is in the near-surface environment where humans, animals, and plants live, (2) leakage and seepage flow processes are coupled, and (3) the main risk drivers are CO_2 flux and concentration. Given these concepts, a rigorous coupled modeling framework is needed to make defensible estimates of CO_2 flux and concentration for potential leakage and seepage scenarios. The results of model simulations can be used to quantify the two key HSE risk drivers, namely seepage flux and near-surface concentrations. The relevant time and length scales for HSE risk assessment that we consider are between 1 month and 10 years, and from 10 m to 1 km, respectively. Over these scales, temporal and spatial averaging of surface-layer properties such as temperature, pressure, and precipitation is defensible. We focus on diffuse leakage and seepage as opposed to catastrophic discharges such as would occur through open boreholes or well blowouts, and we simulate the resulting flow and dispersion processes in the natural hydrogeologic and meteorologic systems.

The coupled modeling framework is built on the integral finite difference multiphase and multicomponent reservoir simulator TOUGH2. The new coupled modeling framework is called T2CA which stands for TOUGH2 for CO_2 and Air. T2CA models CO_2 and air in both subsurface and atmospheric surface-layer regions simultaneously. The surface-layer modeling assumes CO_2 dispersion is passive (i.e., not density-dependent) and uses the logarithmic time-averaged wind profile and advective-dispersive transport equation. The logarithmic wind profile is generated by suitable choice of boundary conditions and medium properties in the surface layer. Surface-layer dispersivities are calculated from the Pasquill-Gifford curves and Smagorinski Model for large scale and sub-grid scale atmospheric dispersion, respectively. We have verified the coupled modeling framework in terms of physical property estimates, surface-layer transport and dispersion, and transition from passive to active flow and observed very good agreement in comparison studies.

Application of the model to a thick unsaturated zone system with varying properties showed the dependence of CO_2 seepage and near-surface CO_2 concentrations on leakage flux and other system properties. In general, we found that the model unsaturated zone has a limited capability to attenuate CO_2 leakage flux, and CO_2 concentrations can be quite large in the shallow subsurface. Large CO_2 concentrations in the shallow subsurface would pose substantial risk to plants by inhibiting root respiration. Demonstrations of the model for a problem with full subsurface–surface-layer coupling show the large dispersion and dilution expected in the atmospheric surface layer. Whereas CO_2 concentrations in the subsurface can be high, in the surface layer the wind overwhelms the seepage flux and reduces CO_2 concentrations to very low levels. We have also observed the reflux of CO_2 by infiltrating rainwater containing dissolved CO_2, a process that shows the importance of using a coupled modeling framework. Finally, we compared downwind concentrations for 2-D and 3-D simulations of surface-layer dispersion and observed approximately a factor of two decrease in CO_2 concentration for the 3-D simulation relative to the 2-D simulation.

To demonstrate the framework, we have applied T2CA to calculate CO_2 concentrations in the near-surface environment resulting from leakage and seepage associated with the potential use of the Rio Vista Gas Field, California, as a site for geologic CO_2 storage. The Rio Vista Gas Field is a promising location for geologic CO_2 storage by virtue of its location near CO_2 sources in the San Francisco Bay Area, its proven record of natural gas (CH_4) containment, and its depletion due to CH_4 production totaling 3 Tcf (9×10^{10} m^3) to date. The capacity of reservoirs at Rio Vista is estimated to be approximately 3.3×10^{11} kg of CO_2 based on cumulative CH_4 production. Gas is produced from sandy reservoirs separated by thick shale sequences from a depth of approximately 4000 ft (1200 m). The gas traps are described as faulted-dome or up-dip fault traps in an elongated and faulted dome. The west-dipping Midland fault strikes northwest through the eastern portion of the Rio Vista Gas Field.

The sparsely populated Rio Vista area consists of grassy upland and extensive lowland areas and diked-off sub-sea-level islands. The water table depth is less than approximately 7 ft (2 m) over the lowlands, and up to 42 ft (13 m) below ground surface in the highest Montezuma Hills. Precipitation amounting to approximately 18 in yr^{-1} (46 cm yr^{-1}) falls primarily in the winter months. Wind in the area is very steady and strong, and currently supports the largest wind farm in California.

We present results from T2CA of dispersion in the surface layer of CO_2 that discharges at the surface from an area along the Midland fault. For seepage out from the Midland fault zone at a rate of 10^{-4} kg m^{-2} s^{-1}, we observe very strong dispersion associated with surface-layer winds. Carbon dioxide concentrations do not even exceed ambient CO_2 concentrations one meter above the ground surface. In general, the sand-shale sequences and associated reservoir trapping structures at the Rio Vista Gas Field are expected to provide effective storage for injected CO_2. If leakage and seepage were to occur by some unanticipated process, surface-layer winds appear to be a favorable feature of the Rio Vista area for minimizing potential HSE risks at and above the ground surface. However, subsurface CO_2 concentrations can potentially be high with corresponding risk to plant roots and to humans and other animals in subsurface structures such as basements or utility vaults.

The coupled modeling framework T2CA provides a rigorous simulation capability, the application of which can show defensible dispersion and dilution of CO_2 in the surface layer. We recommend extending and enhancing CO_2 leakage and seepage simulation capabilities through development of (1) dense-gas flow surface-layer capabilities for calm conditions, (2) high-flux discharge and inertia-driven flow and dispersion capabilities applicable to well blowouts and other catastrophic leaks, (3) coupling of subsurface flow and transport to buildings and basements, (4) well-bore flow simulation for modeling leakage up open boreholes, and (5) additional case study applications at Rio Vista and other sites.

2.1.3.6 Experimental

2.1.3.6.1 Key Concepts

The methodology and structure of the coupled modeling framework we are using is based on the following key concepts: (1) the human, plant, and animal receptors span the interface between the subsurface and surface layer; (2) the flow processes involved in leakage and seepage are coupled; and (3) the main risk drivers are CO_2 flux and concentration. Before describing the methods and structure, we elaborate on these three key concepts and discuss the time and length scales appropriate to our approach.

First, HSE risk assessment applies to humans, plants, and animals. These environmental receptors live generally near the ground surface but may be entirely below, entirely above, or in both regions at different times. As examples of the importance of the subsurface, surface-layer, and in-between environments, consider the house and basement and the burrowing animals of Figure 2.1.3.4(1). Clearly the house and the burrow are open to gas flow from both the subsurface and surface layers and therefore CO_2 in either the subsurface or surface layer has the potential to affect the environment in which people or animals live. The plants and trees and their roots similarly will be affected by CO_2 leakage and seepage in both the subsurface and surface-layer environments. Because exposure to CO_2 in the near-surface environment is the main risk associated with CO_2 leakage and seepage, we have developed a coupled modeling framework that focuses on this region.

Second, CO_2 leakage and seepage are coupled transport processes. Specifically, CO_2 gas in the near-surface environment will flow by advection and diffusion as controlled by pressure, density, and concentration gradients. For example, seeping CO_2 will be strongly advected by surface winds above the ground surface, while atmospheric pressure variations (i.e., barometric pumping) will cause CO_2 to move in and out of the subsurface. However, the low permeability of the subsurface will tend to dampen advective transport driven by pressure variations and wind in the surface layer. Rainfall and associated infiltration containing dissolved CO_2 can be another mechanism for CO_2 to return from the surface layer to the subsurface. Because of these apparent coupled processes occurring between the surface layer and subsurface, a coupled modeling framework capable of modeling these interactions is required.

Third, if high CO_2 concentrations are the fundamental adverse condition for HSE risk, then CO_2 seepage flux and near-surface CO_2 concentration are the main risk drivers. Seepage flux in terms of mass has units of kg CO_2 m^{-2} s^{-1} and is a measure of the rate at which CO_2 is passing out of the ground per unit area. If CO_2 is the only component of the gas stream seeping out of the ground, then flux and concentration are directly correlated. However, if the CO_2 is contained within a stream of another component (e.g., with steam in a geothermal system vent or geyser), then there can be a high CO_2 flux with low CO_2 concentrations. In this sense, flux and CO_2 concentration must be considered independently. In the case where the only component in the seeping gas is CO_2, the seepage flux is a good indicator of whether the given winds, surface water flows, or plant uptake rates are capable of reducing CO_2 concentrations to safe levels. As for CO_2 concentrations, the location of the occurrence of high concentration and nature of the receptor control the attendant risk. For example, high CO_2 concentrations at a depth of 1 m in the ground may cause negligible risk to humans because they are living on the ground surface, while such concentrations would pose a serious risk to plants through exposure to plant roots.

Given these key concepts, it is apparent that a rigorous and quantitative coupled modeling capability is required to make defensible estimates of CO_2 flux and concentration for various expected leakage and seepage scenarios. Simplified models of the subsurface or surface layer alone may not stand up to public and scientific scrutiny. We have used a methodology and structure that is based on multiphase and multicomponent reservoir simulation. The fluxes and concentrations calculated by the coupled framework can be used as inputs to exposure models to calculate defensible HSE risks. The direct output from the present coupled modeling framework is also useful by itself since CO_2 flux and

concentration are primary risk drivers. The approach we have taken can be used to model the whole leakage pathway from deep sequestration site to the surface, but here we focus the model description on the region where the main HSE hazards occur, namely the near-surface environment containing the unsaturated zone and surface layer.

2.1.3.6.2 Length and Time Scales

With CO_2 storage and sequestration operations potentially occurring on a large and widespread industrial scale, the length and time scales of interest to CO_2 risk characterization are quite large. Because broad and diffuse CO_2 seepage may occur over large areas for long periods of time, such leakage and seepage may be hard to detect and difficult to mitigate. As such, diffuse seepage is an important focus for risk assessment and risk management. Catastrophic events such as well failures are also relevant, but such events are obviously serious HSE risks and everything possible will be done to stop such events. We have focused on the 10 m to 10^3 m length scale, and the 1 month to 10 year time scale. Over these length and time scales, averaging is defensible. For example, constant wind speed, pressure, infiltration, and other weather-related processes can be used since the time scale is relatively long. On shorter time scales, one would need to use variable weather and seasonal conditions. While the coupled model is capable of nonisothermal simulations, we have considered only isothermal situations to date and we make use of a stability class parameterization to model temperature-related instability and its effect on atmospheric dispersion.

2.1.3.6.3 Subsurface Flow and Transport

The coupled modeling framework we are using is built on the TOUGH2 code (Pruess et al., 1999), a multiphase and multicomponent integral finite difference reservoir simulator. Briefly, TOUGH2 uses a multiphase version of Darcy's law for fluid flow and the advective-dispersive model for component transport. Readers interested in greater detail and information on the theory or practical implementation of TOUGH2 should consult the users guide (Pruess et al., 1999) and the website (http://www-esd.lbl.gov/TOUGH2). The coupled model is based on an extension of the EOS7R module (Oldenburg and Pruess, 1995; Pruess et al., 1999), and handles five components (H_2O, brine, CO_2, a gas tracer, air) and heat. Air is a pseudocomponent that is approximated as a mixture of 21% oxygen and 79% nitrogen by volume. Real gas mixture properties are calculated so the full range from high-pressure sequestration-site conditions to low-pressure ambient surface-layer conditions can be modeled. We refer to the coupled model as T2CA, for TOUGH2 for CO_2 and Air. While the discussion below focuses on the CO_2 transport, all of the gas-phase components are modeled in the TOUGH2 multicomponent framework, and an analogous treatment can be developed for heat.

2.1.3.6.4 Atmospheric Dispersion

The approach we use for atmospheric surface-layer transport is based on well-established large-scale atmospheric dispersion methods. In essence, our approach uses parameterized dispersivities derived for the atmospheric surface layer along with a logarithmic velocity profile representing time-averaged surface winds to model advection and dispersion in the surface layer (Slade, 1968). The parameterized dispersivities come from the Pasquill-Gifford (Pasquill, 1961; Gifford, 1961) curves defined for six different atmospheric stability values (P-G classes A–F) where class A is extremely unstable and class F is moderately stable. An additional dispersivity to model sub-grid scale dispersion near the ground known as the Smagorinski Model (SM) is also included (Arya, 1999). The surface layer is defined simply by setting porosity to unity and permeability to a range of values orders of magnitude larger than the subsurface parts of the domain and which specify the desired logarithmic profile for the given boundary conditions. The entire coupled subsurface–surface-layer calculation is carried out using a single grid. Hence, the model regions are implicitly coupled. Full multiphase and multicomponent flow and transport are used throughout the domain. Depending on how the user defines the properties of the domain, the model can be run as subsurface only, surface layer only, or

coupled subsurface–surface-layer. Additional layers and materials can be added to represent details such as plants, leaf litter, and soils as information about the effects of these materials becomes known. The approach is described in detail in Oldenburg and Unger (2003b).

Field experiments of dense gas dispersion have been used to develop correlations involving the most important parameters controlling atmospheric dispersion such as wind speed, density of released gas, and release flux (Britter, 1989; Britter and McQuaid, 1988). These correlations were developed based on simple scale and dimensional analyses. One of these correlations relates the seepage flux and average wind speed at an elevation of 10 m to the form of the dispersion process, i.e., whether it is active (density-dependent) or passive as appropriate for a gas tracer. In Figure 2.1.3.6.4(1), we have plotted this correlation with values appropriate for CO_2-air mixtures for various source area length scales along with the typical flux of CO_2 emitted and taken up by plants, soil, and roots known as the net ecosystem exchange (NEE) (e.g., Baldocchi and Wilson, 2001). As shown in Figure 2.1.3.6.4(1), seepage fluxes have to be quite high (note logarithmic scale) for windy situations for the resulting dispersive mixing process to be active. Note that wind conditions are averages over a period of 10 minutes.

In prior work (Oldenburg et al., 2002a; Oldenburg and Unger, 2003c), we have simulated subsurface migration of leaking CO_2 through the unsaturated zone with rainwater infiltration for various leakage rates specified at the water table. These leakage rates were given as annual mass leakage percentages of the total stored CO_2. Typical seepage fluxes for the 0.1% yr^{-1} leakage rate were on the order of 10^{-5}–10^{-6} kg m^{-2} s^{-1}. As shown in Figure 2.1.3.6.4(1), seepage fluxes of this magnitude lead to passive dispersion for all but the calmest wind conditions.

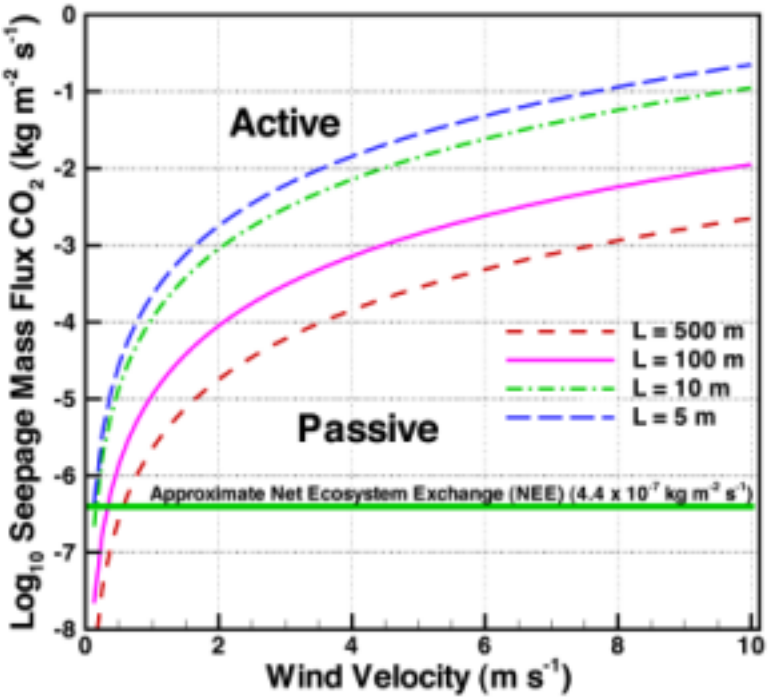

Figure 2.1.3.6.4(1). Correlation for active (i.e., density-dependent) and passive dispersion in the surface layer as a function of seepage flux and wind speed for four different source length scales.

2.1.3.7 Results and Discussion

2.1.3.7.1 Introduction

In this section, we present results of applications of the coupled model T2CA to various problems related to CO_2 leakage and seepage. Because of the lack of available experimental or numerical results for coupled subsurface–surface-layer CO_2 flow and transport, we have compared results of specific components of the model against available independent data and simulation results. For example, we have compared physical properties of the gas mixtures in T2CA against independent predictions from a database of the National Institute of Science and Technology (NIST) and observed good agreement. We have also compared our surface layer dispersion results against a commercial fluid dynamics code called FLUENT (http://www.fluent.com/) that solves the complete Navier-Stokes equations for density-dependent gas flow and observed good agreement. And finally T2CA results show a transition to active flow very close to that predicted by the experimental correlations of Britter and McQuaid (1988). Taken together, the agreement of our model with other data and models for its various components provides a significant level of confidence of the coupled model. For further details of these verification studies, see Oldenburg and Unger (2003b).

2.1.3.7.2 Unsaturated Zone Attenuation

The purpose of this application was to examine the extent to which the unsaturated zone can attenuate CO_2 leakage, full details of which can be found in Oldenburg et al. (2002a) and Oldenburg and Unger (2003c). The system we consider consists of a thick (30 m) unsaturated zone into which a CO_2 leakage flux is released from below. The leakage fluxes are arbitrarily set by prescribing annual losses of 0.1%, 0.01%, and 0.001% by mass of a 4×10^9 kg CO_2 storage reservoir corresponding to fluxes of 4.04×10^{-8}, 4.04×10^{-7}, and 4.04×10^{-6} kg m^{-2} s^{-1} if the leakage occurs over a 100 m radius region. The leakage area was one of the many properties of the system that was varied as part of the sensitivity analysis discussed below. Rainfall infiltration flows downward through the section and acts to dissolve CO_2 and transport it downward. Additional properties of the system for the base case are provided in Table 2.1.3.7.2(1).

Figure 2.1.3.7.2(2) shows the steady-state simulation results for the base case at the three different leakage rates. Carbon dioxide concentrations in the shallow subsurface increase with increasing leakage rate, as diffusion and the specified rainfall infiltration are overwhelmed by larger leakage fluxes. Note further the limited degree to which the CO_2 spreads outward in the unsaturated zone despite the density contrast. Pressure gradients induced by the active leakage flux dominate over gravity effects here and thus lead to vertical CO_2 flow through the vadose zone to the ground surface (Oldenburg and Unger, 2003c).

Figure 2.1.3.7.2(3) shows plots of seepage flux and near-surface CO_2 concentration (mole fraction) summarizing a large number of simulations carried out as part of a sensitivity analysis (Oldenburg and Unger, 2003c). For reference, we have plotted the CO_2 net ecosystem exchange (NEE) 4.4×10^{-7} kg m^{-2} s^{-1} (Baldocchi and Wilson, 2001) and the soil-gas CO_2 mole fraction ($x_{gas}^{CO2} = 0.3$) that has caused tree mortality by root suffocation (Farrar et al., 1995). As shown, the leakage flux exerts the strongest control on flux and concentration at the ground surface. Permeability and permeability anisotropy are also very important in controlling CO_2 seepage flux and near-surface concentrations. The fundamental observation from these simulations is that subsurface CO_2 concentrations from leakage and seepage can be high in the near-surface environment, even when the fluxes are of the same order of magnitude as the NEE (Oldenburg and Unger, 2003c).

Table 2.1.3.7.2(1). Hydrogeological properties of the unsaturated zone for the base case.

Property	Value
Permeability ($k_r = k_Z$)	1 x 10^{-12} m^2 (1 Darcy)
Porosity (ϕ)	0.2
Infiltration rate (i)	10.0 cm yr^{-1}
Residual water saturation (S_{lr})	0.1
Residual gas saturation (S_{gr})	0.01
van Genuchten (1980) α	1 x 10^{-4} Pa^{-1}
van Genuchten (1980) m	0.2

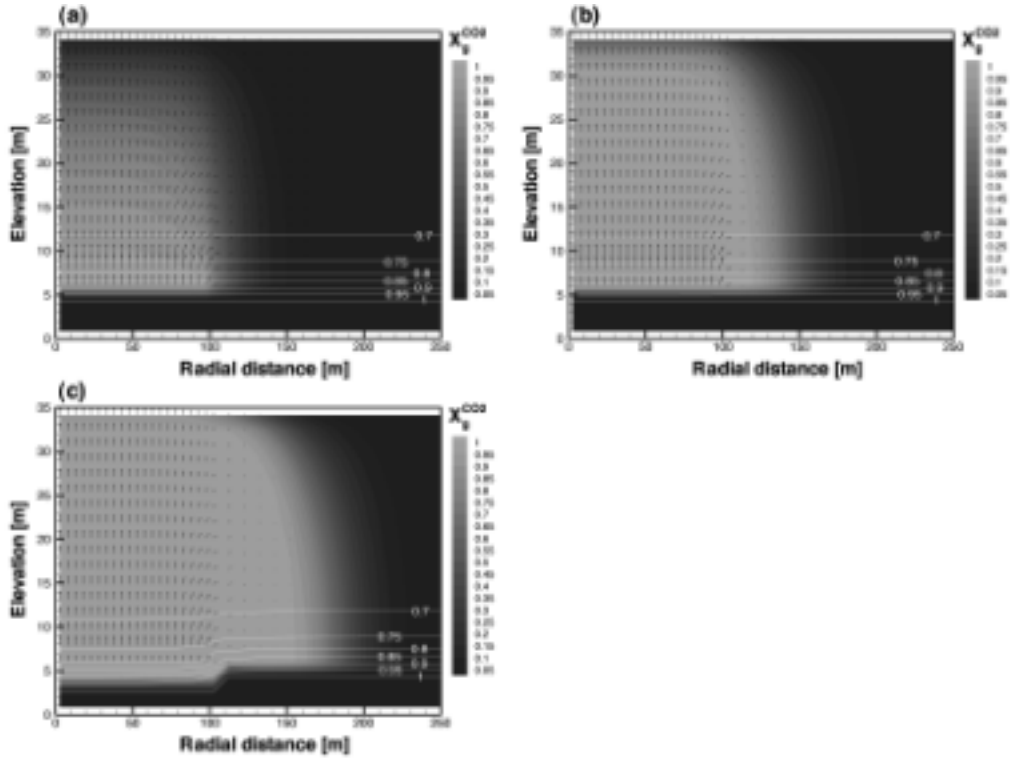

Figure 2.1.3.7.2(2). Simulation results for leakage in a thick unsaturated zone where shading indicates mass fraction of CO_2 in the gas phases, and labeled contour lines indicate water saturation, and vectors show gas phase pore velocity for steady-state leakage rates of 4 x 10^4, 4 x 10^5, and 4 x 10^6 kg yr^{-1}. The maximum vector size represents values of approximately (a) 0.057, (b) 0.53, and (c) 3.6 m d^{-1}.

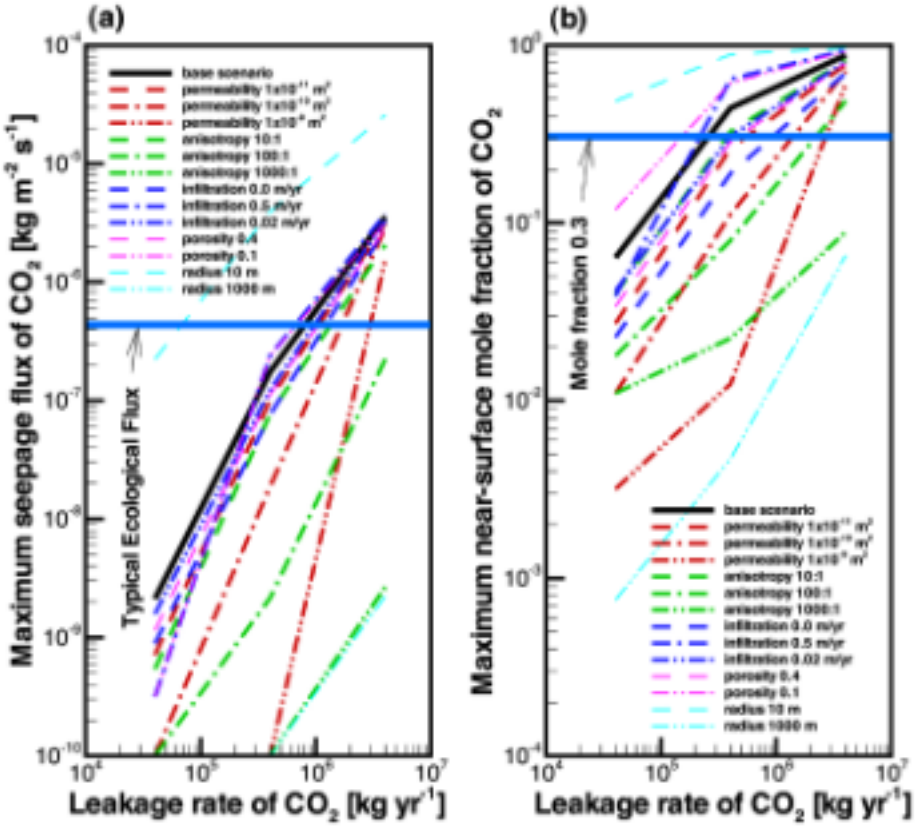

Figure 2.1.3.7.2(3). Maximum seepage flux of CO_2 and maximum near-surface gas mole fraction CO_2 as a function of leakage rate at steady-state seepage conditions.

2.1.3.7.3 Subsurface–Surface-Layer Coupling

We have also applied the new simulation capability to the coupled subsurface–surface-layer system, properties of which are listed in Table 2.1.3.7.3(1). The domain discretization and boundary conditions are shown in Figure 2.1.3.7.3(2). Further details of this application can be found in Oldenburg and Unger (2003a, b, d). We present in Figure 2.1.3.7.3(3) simulation results showing subsurface and surface layer CO_2 concentrations (mass fraction) and gas-phase velocity vectors for the cases of winds of 1 m s^{-1} and 5 m s^{-1} at a height of 2 m from the ground surface and stable (Pasquill-Gifford (P-G) Class F) and unstable (P-G Class A) atmospheric conditions (e.g., Pasquill, 1961; Gifford, 1961). It is important to note that in all of the simulations we have assumed a zero background CO_2 concentration to emphasize the additional CO_2 that seeps from the ground in the various scenarios. Note the downward migration of CO_2 into the subsurface due to its dissolution in infiltrating water at 10 cm yr^{-1}. Note also the mass fraction scale in Figure 2.1.3.7.3(2) shows that CO_2 concentrations in the surface layer are very low, barely above the background concentration of 370 ppmv which would be 0.0056 by mass fraction. The fundamental conclusion is that surface winds and atmospheric dispersion are very effective at diluting CO_2 seepage fluxes. However, calm conditions and topographic depressions not yet analyzed are moderating effects that can allow larger CO_2 concentrations to develop.

Given that HSE risks will be calculated based on exposures at certain locations in the flow field, we have made a preliminary analysis of the dependence of downwind CO_2 concentrations as a function of wind speed and height above the ground surface for the test problem. Shown in Figure 2.1.3.7.3(4) are values of CO_2 mass fraction in the surface-layer as a function of Pasquill-Gifford stability class for two different average ambient winds. As shown, the downwind concentrations depend mostly on wind speed and stability class. Wind speed increasing by a factor of five causes CO_2 mass fractions to decline by approximately a factor of seven. With increasing atmospheric stability, the downwind concentration can be expected to increase by approximately a factor of five. Because dispersion is strong in all cases, the concentrations depend less strongly on height above the ground. The results shown above are for 2-D systems. The coupled modeling framework is a fully 3-D capability, limited only by computer resources and other practical data handling issues insofar as problem size is concerned. In 3-D simulations presented in Oldenburg and Unger (2003b), CO_2 concentrations were reduced by approximately a factor of two at downstream locations relative to the 2-D case, a result explained by lateral dispersion not included in 2-D simulations.

Table 2.1.3.7.3(1). Properties of the coupled subsurface–surface-layer model system.

Property	Value
Subsurface	
Subsurface region extent (x x y x z)	1 km x 1 m, 0 m < z < 35 m
Discretization (Nx x Ny x Nz)	100 x 1 x 35
Permeability ($k_X = k_Z$	1 x 10^{-12} m^2
Porosity (ϕ)	0.2
Infiltration rate (i)	10. cm yr^{-1}
CO_2 flux region	450 m < x < 550 m
CO_2 mass flux	4.04 x 10^{-6} kg m^{-2} s^{-1}
Residual water sat. (S_{lr})	0.1
Residual gas sat. (S_{gr})	0.01
van Genuchten (1980) α	1 x 10^{-4} Pa^{-1}
van Genuchten (1980) m	0.2
Surface Layer	
Surface-layer region extent (x x y x z)	1 km x 1 m, 35 m < z < 45 m
Discretization (Nx x Ny x Nz)	100 x 1 x 20
Pressure in surface layer	1 bar
Temperature (isothermal)	15 °C
Pasquill-Gifford stability class	F
Velocity profile	logarithmic
Reference velocity at z = 10 m	0, 1, or 5 m s^{-1}
Friction velocity for u_x = 1 m s^{-1}	0.0868 m s^{-1}
Friction velocity for u_x = 5 m s^{-1}	0.434 m s^{-1}
Reference height (z_0)	0.10 m

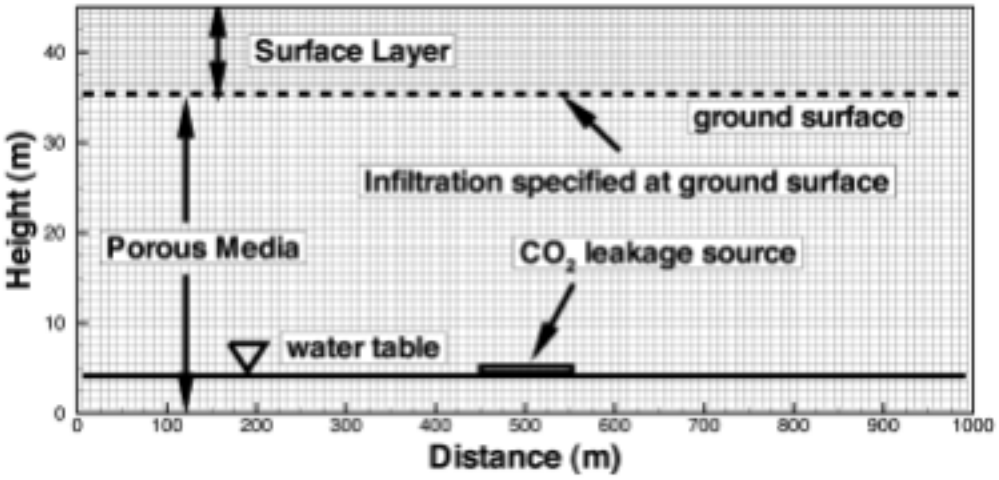

Figure 2.1.3.7.3(2). Domain and discretization used in the coupled subsurface–surface-layer test problem.

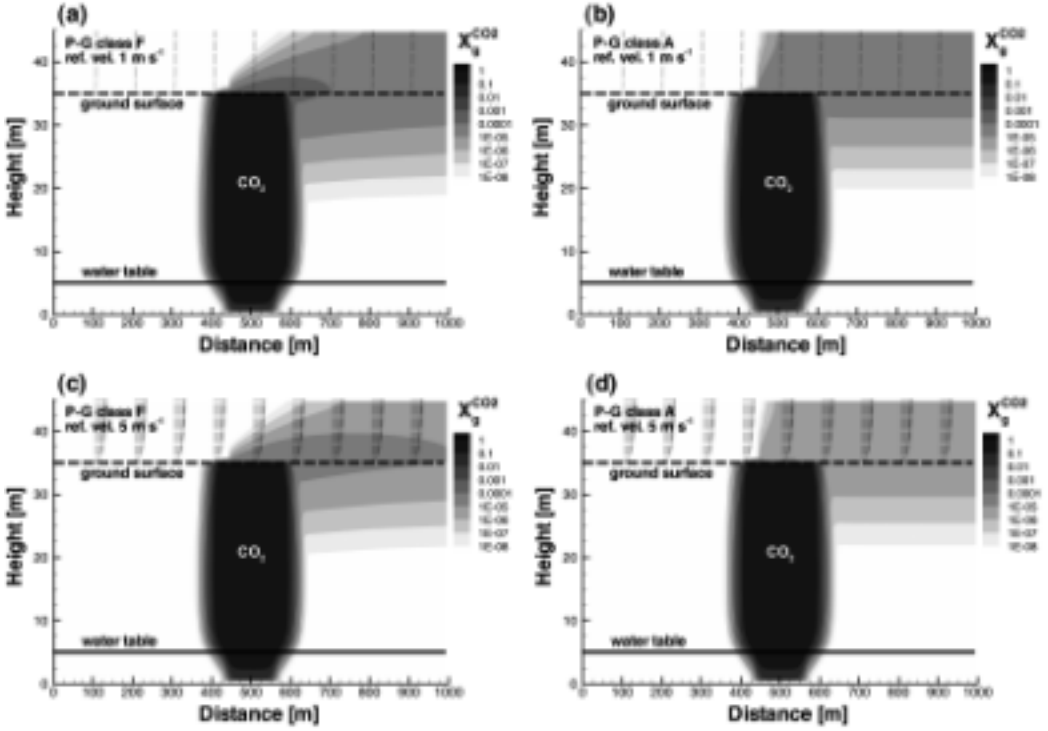

Figure 2.1.3.7.3(3). Simulation results for coupled subsurface–surface-layer problem showing mass fraction of CO_2 in the gas phase and gas velocity vectors. (a) P-G class F, wind speed 1 m s^{-1}; (b) P-G class A, wind speed 1 m s^{-1}; (c) P-G class F, wind speed 5 m s^{-1}; (d) P-G class A, wind speed 5 m s^{-1}.

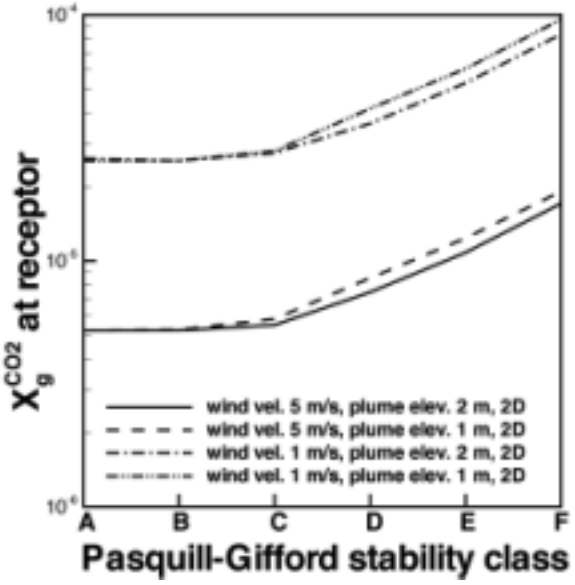

Figure 2.1.3.7.3(4). Concentration (CO_2 mass fraction) at a point 100 m downwind from the seepage source for various atmospheric and wind conditions.

2.1.3.7.4 Preliminary Application

2.1.3.7.4.1 Rio Vista Gas Field

In continuous production since 1936, the Rio Vista Gas Field is the largest onshore gas field in California (Burroughs, 1967). Because it is located near large sources of anthropogenic CO_2 from refineries and power plants serving the San Francisco Bay Area, the Rio Vista Gas Field is a promising candidate for CO_2 Storage with Enhanced Gas Recovery (CSEGR) (e.g., Oldenburg et al., 2001). Natural gas production from the Rio Vista Gas Field peaked in 1951 with annual production of 4.4 x 10^9 m^3, and has declined steadily since then (Cummings, 1999). Based on the cumulative production of CH_4 in excess of 3 Tcf (9.3 x 10^{10} m^3), and assuming the reservoir pressure can be maintained at 122 bars, 65 ˚C, we estimate the Rio Vista Gas Field could hold 3.3 x 10^{11} kg of CO_2. The 680 MW gas-fired power plant located in Antioch, California, 20 km from Rio Vista, is a potential source of CO2. This plant produces 2.2 x 10^9 m^3 (1 bar, 15.5 ˚C) or 4.15 x 10^9 kg (4.15 MT) of CO_2 annually. Thus, the Rio Vista Gas Field could potentially store 80 years of CO_2 output from the power plant.

In this section, we present a preliminary application of the surface-layer modeling capabilities of T2CA. Details of this application along with a subsurface component can be found in Oldenburg et al., (2003a), while a fully coupled application of T2CA for an actual site remains as future work. Although quite general, the scenario we model is based on actual wind conditions. Because the land use, geologic, hydrologic, and meteorologic, conditions of an area of interest can affect subsurface CO_2 flow, above-ground CO_2 dispersion, and resulting potential hazard to humans, other animals, and the environment, we present a summary of the site conditions below that are used to guide development of the model system.

2.1.3.7.4.2 Site Characterization

The Rio Vista Gas Field is located in the southwest portion of the Sacramento Valley shown in Figure 2.1.3.7.4.2(1). To the east and west of the Sacramento River, the field underlies sub-sea level islands and the Montezuma Hills, respectively. Land use in the area is predominantly agricultural, grazing

lands, or rural open space. The city of Antioch southwest of the study area is the most developed area shown on Figure 2.1.3.7.4.2(1). The towns of Rio Vista, Isleton, and Walnut Grove (year 2000 populations of 4727, 829, and 910, respectively) are largely residential, with minor commercial and industrial areas.

The primary gas reservoir in the Rio Vista Gas Field is the Eocene Domengine sand, a predominantly marine sandstone with shale interbeds, located at approximately 1200 m depth (4000 ft). In Figure 2.1.3.7.4.2(2), we show a highly schematic cross section (not to scale in the vertical direction) that shows the general structure of the reservoir and overlying formations. The west-dipping Midland fault strikes northwest through the eastern portion of the Rio Vista Gas Field. Stratigraphic units at the reservoir level exhibit normal (down to the west) displacement, and thicken across this fault from east to west indicating syndepositional faulting. The Midland fault and associated faults were likely due primarily to extensional tectonics during deposition of the reservoir units. The geologic structure in the gas field consists of an elongated, faulted dome (Burroughs, 1967; Johnson, 1990).

Depth to the water table in the area varies from less than 2 m (7 ft) at lower elevations, to greater than 13 m (42 ft) in or near the Montezuma Hills. The maximum horizontal gradient of the water table is approximately 0.003 outward from the Montezuma Hills, while horizontal gradients are much less in the lowlands characterized by flat topography and perennial water channels. Extensive wetlands and slough channels cover much of the area between diked-off islands developed for agriculture. The sub-sea level islands are former wetlands that have been drained and diked off from water channels for agriculture. The only perennial streams in the Montezuma Hills occupy some of these drainages. Minor seasonal streams drain the margins of the hills to the north and west.

The study area can be divided topographically into the (1) lowland and (2) upland areas located east and west of the Sacramento River, respectively. The majority of the study area east of the Sacramento River consists of flat lowlands near or below sea level (minimum elevation of –4.6 m (–15 ft). Sub-sea level islands were formed by levees along the Sacramento and San Joaquin Rivers, and associated sloughs in the Sacramento-San Joaquin River delta. Upland areas are also relatively flat, although they include the Montezuma Hills, an area of low-lying hills west of the Sacramento River with a maximum elevation of 89 m (293 ft).

The climate of the study area is sub-humid. Mean annual precipitation, primarily rain, is 400 to 500 mm (16 to 20 inches) and mean annual temperature is 14 to 17 ºC (58 to 62 ºF) (Miles and Goudy, 1997). The highest mean precipitation rate and lowest temperature occurred in the winter (December-February), with values of 823 mm yr^{-1} (32 inches yr^{-1}) and 9 ºC (48 ºF), respectively. Mean spring-time (March-May) precipitation and temperature were 438 mm yr^{-1} (17 inches yr^{-1}) and 14 ºC (57 ºF), while mean fall values were 194 mm yr^{-1} (8 inches yr^{-1}) and 16ºC (61 ºF). Atmospheric pressure at Rio Vista is not subject to large pressure variations such as occur in areas subject to hurricanes, e.g., the U.S. Gulf Coast.

A five-year time series (06-11-97 to 06-12-03) of hourly wind speed and direction measurements at the DWR station on Twitchell Island is shown in the form of a wind rose in Figure 2.1.3.7.4.2(3). In the figure, the radial spokes indicate the direction the wind is coming from, the concentric circles are contours of the percentage of time (in 10% intervals) that the wind blows from the given direction, the thickness of the bar on the spokes indicates the wind speed, and the numbers at the end of the spokes are the total percentage time that the wind blows from the given direction. Over the measurement averaging time of 1 hour, there were no calms recorded. Figure 2.1.3.7.4.2(3) shows that the dominant wind direction in the study area is from the west to west-southwest (i.e., percent occurrence = 29.44 + 24.53 = 54%). The dominant wind directions during the spring (March-May), summer (June-August) and a portion of the fall (September-October) are from the west to west-southwest. However, from November to February, dominant wind directions are highly variable. The highest (4.8 m s^{-1} (10.6 mph)) and lowest (2.6 m s^{-1} (5.7 mph)) mean wind speeds were observed during summer and winter months, respectively, while intermediate mean wind speeds were observed during spring and fall months (3.7 and 2.9 m s^{-1} (8.1 and 6.4 mph), respectively). These windy

conditions have not gone unnoticed, and the Montezuma Hills is the location of the newest and largest wind farm in California, which is expected to produce 162 MWe by the end of 2003.

2.1.3.7.4.3 Scenario for Leakage and Seepage

To demonstrate the application of T2CA for leakage and seepage risk characterization, we present results for a leakage scenario in which we assume that CO_2 migrates up the Midland Fault leading to seepage at the ground surface. This preliminary application demonstrates the surface-layer dispersion part of the model. This focus on the surface-layer component is relevant because the main potential risk to people would be in the town of Isleton, to which CO_2 could be blown by the prevailing weserly winds. In the scenario, we assume a leakage rate of 1% yr^{-1} by mass of the 3.3 x 10^{11} kg CO_2 storage site (i.e., 3.3 x 10^9 kg yr^{-1}) flowing past a cross sectional area of one square km (1.0 x 10^6 m^2, or 100 hectares), which gives rise to a leakage flux of approximately 10^{-4} kg m^{-2} s^{-1}. This approach of selecting an arbitrary leakage rate is necessary because we have no knowledge of any actual processes that would allow the gas reservoir to leak given its proven shale seals and structure that form the natural gas traps. Thus, we specify an arbitrary seepage rate to analyze what the CO_2 concentrations might be given the known dispersive processes in the surface layer if this unexpected leakage and seepage scenario were to occur.

The scenario we model assumes that leaking CO_2 migrates up the Midland fault from depth and spreads laterally until the CO_2 seeps from the ground over a region 1 km wide measured normal to the fault. Properties of the system are presented in Table 2.1.3.7.4.3(1). As shown in Figure 2.1.3.7.4.2(1), the Midland fault is perpendicular to the prevailing southwesterly winds (Figure 2.1.3.7.4.2(3)) and thus amenable to modeling in two dimensions. A system with no topographic relief was chosen, consistent with the flat topography of the lowland areas. We present in Figure 2.1.3.7.4.3(2) the discretization and boundary conditions of the surface-layer model domain for the dispersion of CO_2 seeping from the Midland fault.

Typical steady-state results are shown in Figure 2.1.3.7.4.3(3) by the CO_2 concentrations (mass fraction) and wind velocity vectors for P-G class F (Pasquill, 1961; Gifford, 1961) and seepage flux (Q_s^{CO2}) equal to 10^{-4} kg m^{-2} s^{-1} at three different wind speeds. We chose winds of 2 m s^{-1}, 4 m s^{-1}, and 8 m s^{-1} (4.4, 8.8, and 17.6 mph, respectively) to show the variability in CO_2 dispersion with wind speed. Note from Figure 2.1.3.7.4.2(3) that wind speeds greater than 5 m s^{-1} occur approximately 40% of the time on nearby Twitchell Island. As shown in Figure 2.1.3.7.4.3(3), dispersion is very effective at diluting the CO_2 plume in the surface layer. For the less stable atmospheric stability classes (P-G classes A–E), the dispersion will be even more effective. However, rare calm conditions will diminish mixing and dispersion in the surface layer.

Results of a suite of simulations are summarized in Figure 2.1.3.7.4.3(4) which shows the CO_2 mole fraction in the gas (assuming zero background CO_2 concentrations) at a height of 1 m above the ground due to CO_2 seepage and dispersion in the surface layer for three different steady wind conditions at various locations away from the source region. Note the interesting reversal in CO_2 concentration for various stability classes as a function of location. In particular, the midpoint region of the source area has lower concentrations for the most unstable P-G classes A, B, and C. Under more stable conditions, the concentrations are higher at the midpoint and downstream edge of the source than the downstream locations at 0.5 and 1 km. Note that higher winds produce proportionately smaller CO_2 concentrations. Additional simulations not shown here demonstrate the high degree of linearity of this dispersion problem with respect to seepage flux. Specifically, one-tenth and ten times higher seepage fluxes produce one-tenth and ten times higher CO_2 concentrations, respectively. Thus for a case of a 100 m-wide seepage zone along the Midland fault and P-G class F with the same leakage mass flow rate as shown in Figure 2.1.3.7.4.3(2), we estimate that for the most stable atmospheric conditions, CO_2 concentrations could reach values of 0.7% (10 x 7 x 10^{-4}), approximately 20 times the current ambient CO_2 concentration. The overall conclusion from these simulations is that the high winds in the Rio Vista area will generally be very effective at

dispersing CO_2 seepage plumes, which suggests that HSE risks due to seepage under these conditions will likely be small above the ground surface.

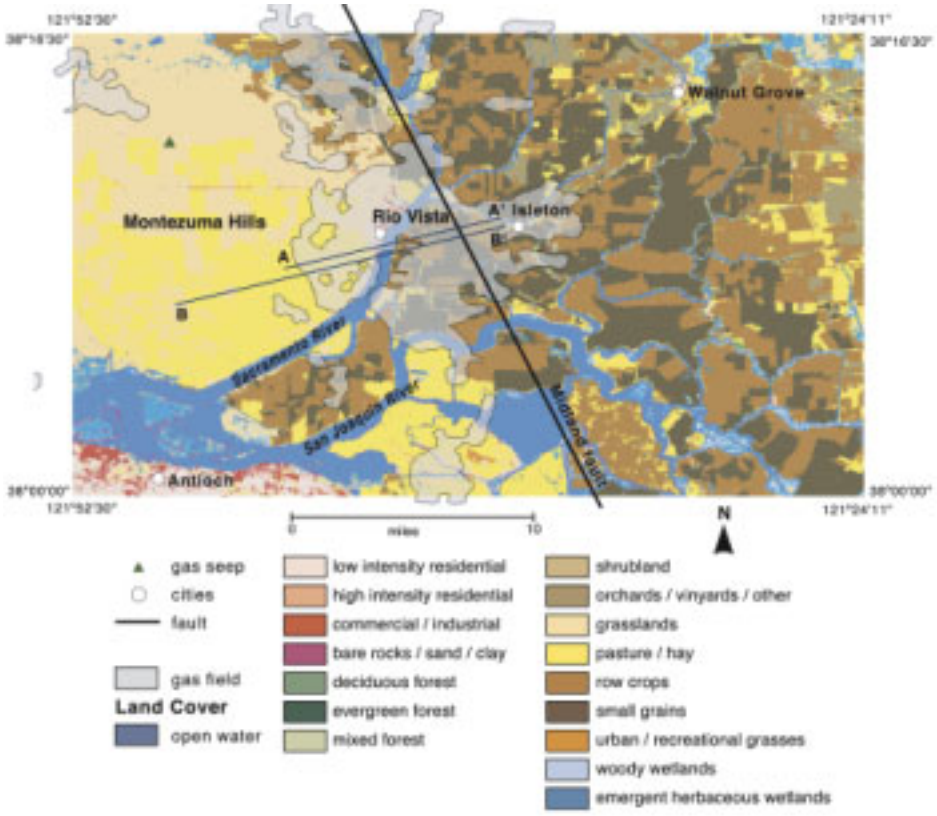

Figure 2.1.3.7.4.2(1). Land cover map of the Rio Vista study area showing land uses. Map is derived from National Land Cover Data 1992 (Vogelmann et al., 2001). Also shown are the location of the Midland fault, gas fields, and cross section lines A-A' and B-B'.

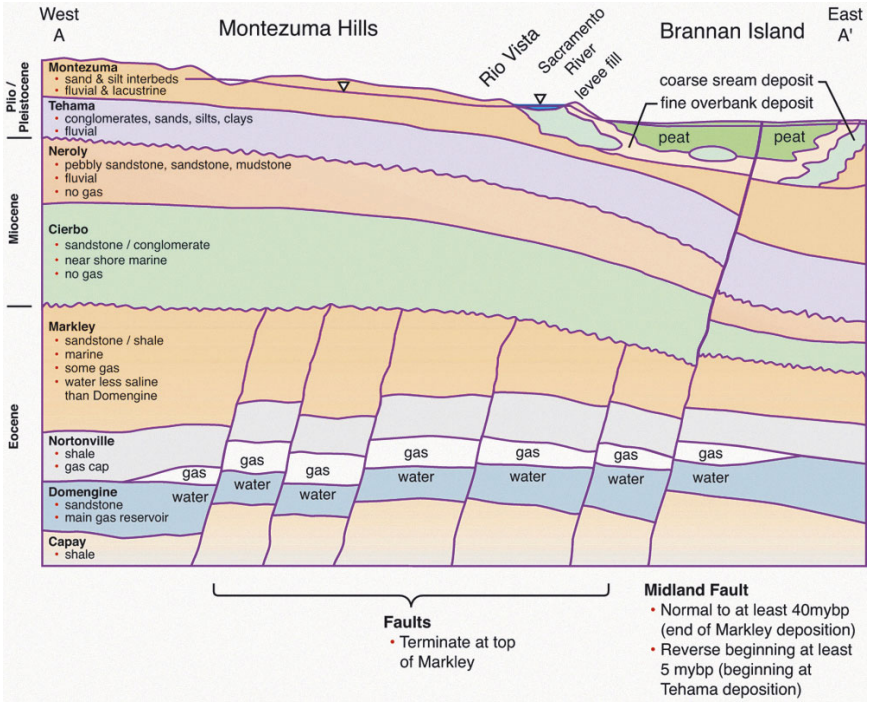

Figure 2.1.3.7.4.2(2). Cross section A-A' of the Rio Vista area. Note that gas reservoir thickness is exaggerated relative to total formation thicknesses.

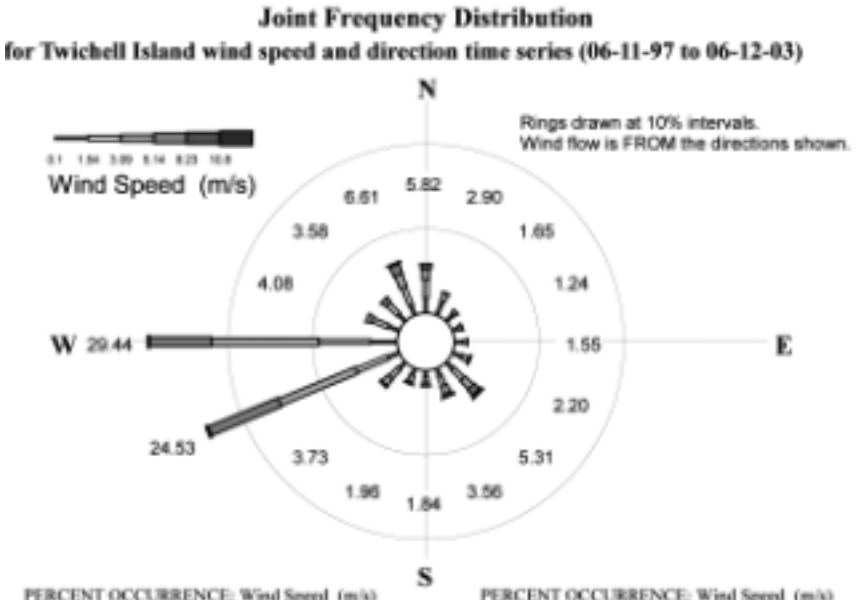

PERCENT OCCURRENCE: Wind Speed (m/s)
LOWER BOUND OF CATEGORY

DIR	0.1	1.54	3.09	5.14	8.23	10.8
N	1.76	2.18	1.19	0.55	0.12	0.01
NNE	1.74	1.00	0.15	0.00	0.00	0.00
NE	1.15	0.47	0.03	0.00	0.00	0.00
ENE	0.79	0.40	0.05	0.00	0.00	0.00
E	1.06	0.46	0.03	0.01	0.00	0.00
ESE	1.18	0.80	0.19	0.04	0.00	0.00
SE	1.11	1.67	1.35	0.81	0.29	0.07
SSE	0.93	1.24	0.95	0.31	0.10	0.02

TOTAL OBS = 49424

PERCENT OCCURRENCE: Wind Speed (m/s)
LOWER BOUND OF CATEGORY

DIR	0.1	1.54	3.09	5.14	8.23	10.8
S	0.76	0.68	0.33	0.07	0.00	0.00
SSW	0.90	0.74	0.25	0.06	0.00	0.00
SW	1.03	1.55	0.92	0.21	0.01	0.00
WSW	1.40	4.10	9.82	8.91	0.30	0.00
W	3.06	6.17	12.66	7.34	0.20	0.01
WNW	1.40	1.99	0.67	0.02	0.00	0.00
NW	1.12	1.75	0.62	0.08	0.00	0.00
NNW	1.25	2.31	1.62	1.22	0.20	0.02

Figure 2.1.3.7.4.2(3). Joint frequency rose diagram for hourly wind speed and direction measurements at the Twitchell Island station from 06-11-97 to 06-12-02.

Table 2.1.3.7.4.3(1). Properties of the Midland fault discharge scenario.

Property	Value
Pressure	1 bar
Temperature	15 °C
Pasquill-Gifford stability class	A–F
Smagorinski parameter (l)	2 m
CO_2 seepage flux region	2500 m < x < 3500 m
CO_2 seepage flux (Q_S^{CO2})	1.0 x 10^{-4} kg m^{-2} s^{-1}
Wind Profile	logarithmic
Reference velocity at z = 2 m	2, 4, and 8 m s^{-1}
Friction velocity for u_x = 2 m s^{-1}	0.70 m s^{-1}
Reference height (z_0)	0.14 m (grown root crops (Slade, 1968))

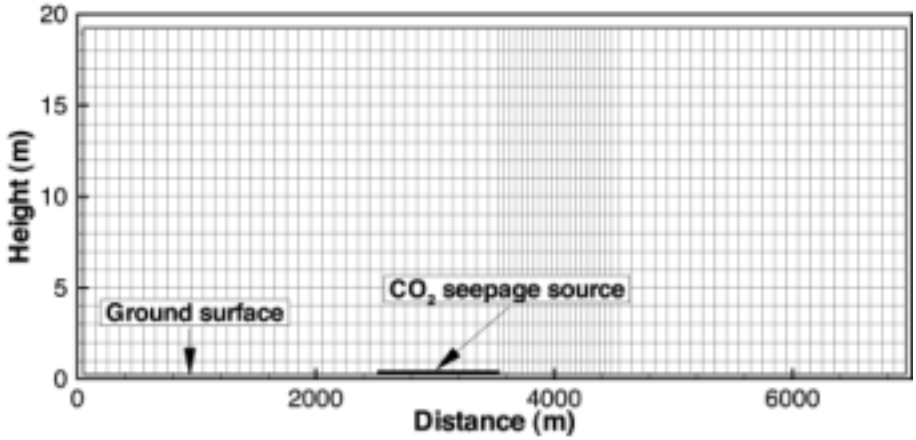

Figure 2.1.3.7.4.3(2). Domain and discretization for the Midland fault discharge problem.

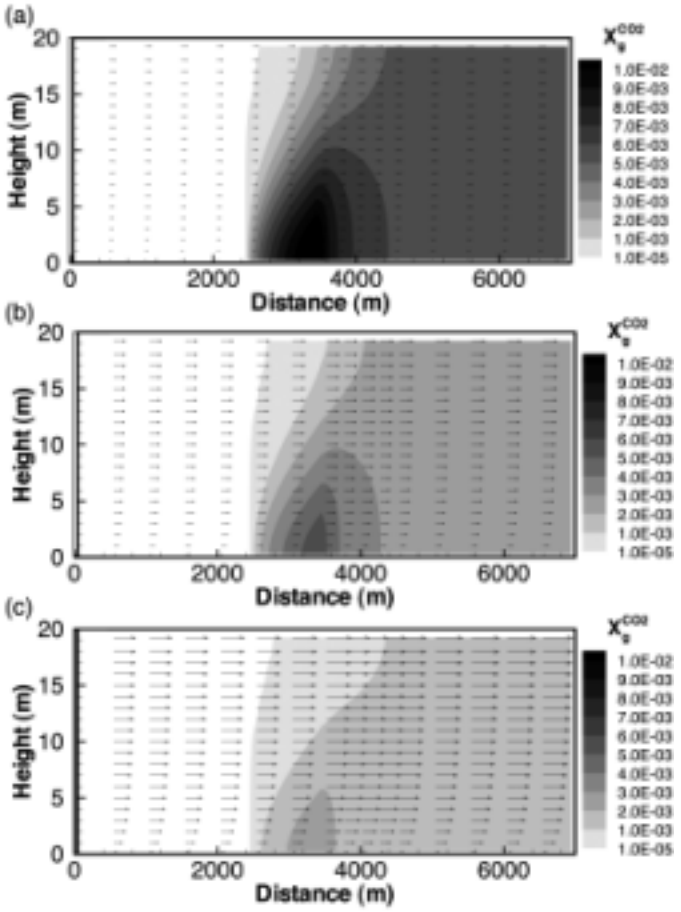

Figure 2.1.3.7.4.3(3). Steady-state gas mass fractions of CO_2 (X_g^{CO2}) and wind velocity vectors for the surface layer dispersion problem for seepage flux equal to 1 x 10^{-4} kg m^{-2} s^{-1} for wind speed equal to (a) 2 m s^{-1}, (b) 4 m s^{-1}, and (c) 8 m s^{-1} for Pasquill-Gifford stability class F.

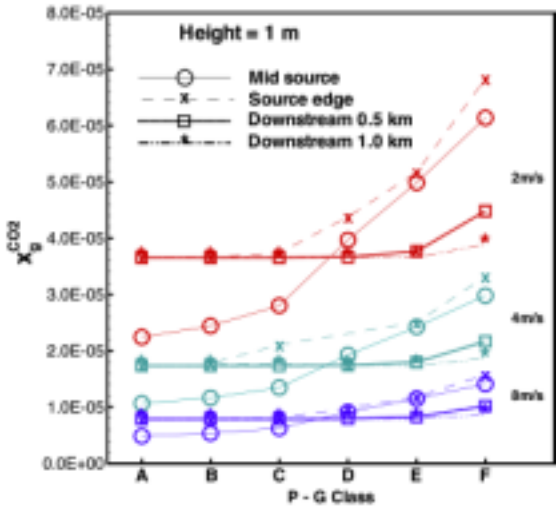

Figure 2.1.3.7.4.3(4). Gas mole fraction CO_2 (x_g^{CO2}) at a height of 1 m for various distances from the source (Mid source is half-way along the source, source edge is at the downstream end of the source, and 0.5 km and 1 km downstream locations are measured from the downstream end of the source) for various Pasquill-Gifford (P-G) Classes.

2.1.3.8 Conclusion

2.1.3.8.1 Main Points

We have demonstrated a coupled modeling framework for modeling CO_2 fluxes and concentrations for risk characterization. This work is relevant and important to the development of geologic carbon sequestration because it provides a rigorous modeling capability for simulating CO_2 flow and transport from the deep CO_2 storage site all the way to the atmosphere. The approach is built on the assumption that the near-surface environment is the main region in which HSE risks will arise. In this region, CO_2 flux and concentration are the main risk drivers. The coupled model handles subsurface and atmospheric surface-layer flow and transport assuming that dispersion in the surface-layer is passive and that the wind is described by a logarithmic velocity profile. Model results show limited unsaturated zone attenuation of leakage flux, with correspondingly large CO_2 concentrations possible in the shallow subsurface. These results show that if leakage leads to CO_2 migrating as far as the vadose zone, high CO_2 concentrations can occur in the root zone of the shallow subsurface with potentially harmful effects on plants, as well as on humans or other animals in poorly ventilated subsurface structures such as basements. Coupled subsurface–surface-layer demonstration simulations show the large degree of dilution that occurs in the surface layer, and the possible reflux of CO_2 to the subsurface that occurs when CO_2 dissolves in infiltrating rainwater. Although no leakage of stored CO_2 would be expected at the Rio Vista Gas Field given its record of natural gas accumulation and production, preliminary application of the model to the site under an assumed seepage scenario suggests that the high and steady winds at Rio Vista are a very favorable feature insofar as they have the potential to disperse CO_2 seepage flux. Details of our studies and preliminary applications can be found in the numerous reports and papers cited throughout this report.

2.1.3.8.2 Recommendations

We recommend development of additional capabilities to contribute to risk characterization. Although the coupled modeling framework T2CA is applicable to many important leakage and seepage scenarios, it is not applicable to absolute calm conditions where active flow (dense-gas dispersion) occurs, nor is it applicable to very high fluxes such as might occur from an open well or catastrophic tank or pipeline release into the open atmosphere. In addition, buildings are neglected even though it is well established that exposures to people by soil-gas contaminants (e.g., radon) are most likely to occur indoors. We recommend that future research funding be directed toward the following:

1) Dense-gas dispersion under calm (i.e., zero wind) conditions. This kind of flow develops under the scenario where there is no wind, and the driving force for advection of CO_2 in the surface layer is the CO_2-air density contrast. Topographic depressions can act as traps for flowing CO_2 in these conditions.

2) High-flux and inertia-driven flows. In the case of a well blowout or surface pipeline or tank leak, high-pressure CO_2 may be discharged. The energy of such a release helps to disperse the discharged CO_2. Modeling of such releases is needed to understand the associated HSE risks.

3) Coupling with buildings. Leaking and seeping CO_2 will enter basements and buildings directly from the subsurface through cracks and unlined floors. Because people spend most of their time indoors, CO_2 concentrations in buildings are important for HSE risk characterization. Simulation capability for risk characterization of basements and other subsurface structures (e.g., utility vaults) is also needed. This component was dropped from the work scope following a mid-project budget cut.

4) Compositional well-bore simulation. Abandoned wells may constitute the single most likely pathway from deep geological storage sites to the near-surface environment. A fully compositional

well-bore simulation capability is needed to model the upward flow of supercritical CO_2, with and without other components, from depth with associated decompression and non-isothermal effects.

5) Additional case study applications. Further simulations and additional cases need to be modeled at Rio Vista, and additional case studies for other potential CO_2 storage projects at other locations should be undertaken to understand the range of outcomes of CO_2 leakage and seepage scenarios.

2.1.3.9 References

Arya, S.P., *Air Pollution Meteorology and Dispersion*, Oxford University Press, 1999.

Baldocchi, D.D. and K.B. Wilson, Modeling CO_2 and water vapor exchange of a temperate broadleaved forest across hourly to decadal time scales, *Ecological Modelling*, *142*, 155-184, 2001.

Britter, R.E., Atmospheric dispersion of dense gases, *Ann. Rev. Fluid Mech.*, *21*, 317–344, 1989.

Britter, R.E and J. McQuaid. *Workbook on the Dispersion of Dense Gases*. Health Saf. Exec. Rep., Sheffield, UK, HSE Contract Research Report No. 17/1988, 1988.

Burroughs, E., Rio Vista Gas Field, Summary of California oil fields, 53, No. 2-Part 2, State of California, Department of Conservation, Division of Oil and Gas, 25, 1967.

Cummings, M.F., *Northern California oil and gas field production, Annual production and well Data, 1977–1998*, State of California, Division of Oil, Gas, and Geothermal Resources, 1999.

Gifford, F.A. Jr., Use of routine meterological observations for estimating atmospheric dispersions, *Nuclear Safety*, *2*, 47–51, 1961.

Johnson, D.S., Rio Vista field-USA, Sacramento basin, Calif., in Foster, N.H., and Beaumont, E.A., eds., *Atlas of oil and gas fields, Structural Traps III*, AAPG Treatise of Petroleum Geology, Atlas of Oil and Gas Fields, Tulsa, Oklahoma, U.S.A., 1990.

Oldenburg, C.M., and K. Pruess, EOS7R: Radionuclide Transport for TOUGH2, Lawrence Berkeley National Laboratory Report *LBNL-34868*, 1995.

Oldenburg, C.M., K. Pruess, and S.M. Benson, Process modeling of CO_2 injection into natural gas reservoirs for carbon sequestration and enhanced gas recovery, *Energy& Fuels*, *15*, 293–298, 2001.

Oldenburg, C.M., A.J.A. Unger, R.P. Hepple, and P.D. Jordan, On Leakage and Seepage from Geologic Carbon Sequestration Sites, Task 1 Report, Lawrence Berkeley National Laboratory Report *LBNL-51130*, July 2002a.

Oldenburg, C.M., T.E. McKone, R.P. Hepple, and A.J.A. Unger, Health Risks from Leakage and Seepage of CO_2 Sequestered in the Subsurface: Requirements and Design of a Coupled Model for Risk Assessment, Task 2 Report, Lawrence Berkeley National Laboratory Report *LBNL-51131*, July 2002b.

Oldenburg, C.M., A.J.A. Unger, and R.P. Hepple, On Atmospheric Dispersion of CO_2 Seepage from Geologic Carbon Sequestration Sites, Task 3 Report, Lawrence Berkeley National Laboratory Report *LBNL-51734,* November 2002c.

Oldenburg, C.M., Y. Zhang, J.L. Lewicki, and P.D. Jordan, Preliminary application of a coupled modeling framework for leakage and seepage at the Rio Vista Gas Field, Task 5 Report, Lawrence Berkeley National Laboratory Report *LBNL-54051*, 2003a.

Oldenburg, C.M., and A.J.A. Unger, Coupled subsurface-surface layer gas transport and dispersion for geologic carbon sequestration seepage simulation, Proceedings of the TOUGH Symposium 2003, Lawrence Berkeley National Laboratory, May 12–14, 2003, and Lawrence Berkeley National Laboratory Report *LBNL-52477*, May 2003a.
http://esd.lbl.gov/TOUGHsymposium/pdfs/OldenburgUnger.pdf

Oldenburg, C.M., and A.J.A. Unger, Coupled Modeling Framework for CO_2 Leakage and Seepage Risk Assessment, Task 4 Report, Lawrence Berkeley National Laboratory Report *LBNL-53009,* June 2003b.

Oldenburg, C.M., and A.J.A. Unger, On leakage and seepage from geologic carbon sequestration sites: unsaturated zone attenuation, *Vadose Zone Journal*, 2, 287–296, 2003c.

Oldenburg, C.M., and A.J.A. Unger, Coupled subsurface-surface layer gas transport and disperison for geologic carbon sequestration seepage simulation, *Vadose Zone Journal*, submitted, 2003d.

Pasquill, F., The estimation of the dispersion of windborne material, *Meterological Magazine*, *90*, 33–49, 1961.

Pruess, K., C. Oldenburg, and G. Moridis, TOUGH2 User's Guide Version 2.0, Lawrence Berkeley National Laboratory Report *LBNL-43134*, 197 pp., November 1999.

Slade, D.H., (editor), *Meteorology and Atomic Energy 1968*, Chapter 2, U.S. Atomic Energy Commission, 1968.

Van Genuchten, M.T., A closed-form equation for predicting the hydraulic conductivity of unsaturated soils, *Soil Sci. Soc. Am. J.*, *44*, 892–898, 1980.

Vogelmann, J.E., S.m. Howard, L. Yang, C.R. larson, B.K. Wylie, N. van Driel, Completion of the 1990's National Land Cover Data Set for the coterminous United States from Landsat Thematic Mapper Data and ancillary data sources, *Photogrammetric Engineering and Remote Sensing, 67*, p. 650-652, 2001.

2.1.3.10 Publications

Oldenburg, C.M., A.J.A. Unger, R.P. Hepple, and P.D. Jordan, On Leakage and Seepage from Geologic Carbon Sequestration Sites, Task 1 Report, Lawrence Berkeley National Laboratory Report *LBNL-51130*, July 2002a.

Oldenburg, C.M., T.E. McKone, R.P. Hepple, and A.J.A. Unger, Health Risks from Leakage and Seepage of CO_2 Sequestered in the Subsurface: Requirements and Design of a Coupled Model for Risk Assessment, Task 2 Report, Lawrence Berkeley National Laboratory Report *LBNL-51131*, July 2002b.

Oldenburg, C.M., A.J.A. Unger, and R.P. Hepple, On Atmospheric Dispersion of CO_2 Seepage from Geologic Carbon Sequestration Sites, Task 3 Report, Lawrence Berkeley National Laboratory Report *LBNL-51734,* November 2002c.

Oldenburg, C.M., and A.J.A. Unger, Coupled Modeling Framework for CO_2 Leakage and Seepage Risk Assessment, Task 4 Report, Lawrence Berkeley National Laboratory Report *LBNL-53009,* June 2003b.

Oldenburg, C.M., Y. Zhang, J.L. Lewicki, and P.D. Jordan, Preliminary application of a coupled modeling framework for leakage and seepage at the Rio Vista Gas Field, Task 5 Report, Lawrence Berkeley National Laboratory Report *LBNL-54051*, 2003a.

Oldenburg, C.M., and A.J.A. Unger, Coupled subsurface-surface layer gas transport and dispersion for geologic carbon sequestration seepage simulation, Proceedings of the TOUGH Symposium 2003, Lawrence Berkeley National Laboratory, May 12–14, 2003, and Lawrence Berkeley National Laboratory Report *LBNL-52477*, May 2003a.
http://esd.lbl.gov/TOUGHsymposium/pdfs/OldenburgUnger.pdf

Oldenburg, C.M., and A.J.A. Unger, On leakage and seepage from geologic carbon sequestration sites: unsaturated zone attenuation, *Vadose Zone Journal*, *2*, 287–296, 2003c.

Oldenburg, C.M., and A.J.A. Unger, Coupled subsurface-surface layer gas transport and dispersion for geologic carbon sequestration seepage simulation, *Vadose Zone Journal*, submitted, 2003d.

2.1.3.11 Bibliography

Style: text to be ‘normal’. ‘Title_6’ thru ‘Title_8’ and ‘table/figure’ can be used within this section

2.1.3.12 List of Acronyms and Abbreviations

Style: text to be 'normal'. 'Title_6' thru 'Title_8' and 'table/figure' can be used within this section

2–D	Two–dimensional
3–D	Three–dimensional
CH_4	Methane
CO_2	Carbon dioxide
FLUENT	A commercial fluid dynamics code.
HSE	Health, safety and environmental (risks)
NEE	Net ecosystem exchange (for CO_2)
NIST	National Institute for Science and Technology
P–G	Pasquill-Gifford
SM	Smagorinski Model
TOUGH2	Reservoir simulator, Transport of Unsaturated Groundwater and Heat 2.
T2CA	for TOUGH2 for CO_2 and Air.
x	mole fraction.
X	mass fraction.